RESEARCH PAPER

Effect of holding time on interfacial evolution and mechanical strength of wide-gap brazed K417G superalloy joints

Xinyu Ren[1] · Hao Wang[1] · Wenwen Li[1] · Qi Dong[1] · Bo Chen[1] · Wei Mao[1]

Abstract

K417G superalloy is widely applied in gas turbine components such as blades, vanes, and nozzles. In this study, wide-gap brazing of K417G superalloy is investigated using BNi-5 filler alloy. The brazing experiment is conducted at 1150 °C for different holding times with the fixed gap of 0.2 mm. For the joints brazed for 15 min, the brazing seam mainly consists of γ/γ' phase, Ni_2Si and TiC phase. The average tensile strength tested at 950 °C is 401 MPa. As the holding time increased, the excessive element diffusion phenomenon is observed. Hence, Ni_2Si intermetallic phases gradually become embedded in the additive alloy particles. The interfacial evolution and fracture behavior are discussed.

Keywords Brazing · Intermetallic compound · Nickel-based superalloys · Diffusion · Microstructure

1 Introduction

Due to the superior high-temperature performance, K417G Ni-based superalloy is widely used in the manufacture of turbine blades, vanes and nozzles in aeronautical industry [1, 2]. For the joining of Ni-based casting superalloys, traditional fusion welding technique has its limitation since higher γ' formers (i.e. Al and Ti) are highly susceptible to hot cracking in the weld metal and heat affected zone (HAZ) [3]. Generally, flexible brazing technique utilizing low melting point filler alloy is commonly used for the brazing and brazing repair of stationary turbine vanes in aero-engines [4, 5]. The lower brazing temperature is attributed to the addition of melting-point-depressants (e.g. Si and B) in the filler alloy. Compared with conventional brazing, wide-gap brazing (WGB) technology was developed in which a blended powder mixture contains filler alloy and additive alloy powders with similar composition with base metal. The WGB technology exploits the mechanism of diffusion brazing, where the strong reaction between filler alloy and base material is achieved via melting, dissolution and diffusion, in bridging larger joint clearances. Meanwhile, the additive alloy provides a capillary path for the molten filler alloy and decreases the amount of the melting point depressants required to fill in the joint [6]. Cheng et al. [7] studied the wide-gap brazing of K417G Alloy with Ni-Co-Cr-Al-Zr-B filler alloy at different joining temperature (i.e. 1100 °C, 1140 °C, 1160 °C 1180 °C, 1200 °C, and 1220 °C). The in-situ precipitation behavior of M_3B_2 boride particles was investigated. The results revealed that the brazing seam was mainly composed of 97.56% equiaxed/spherical $\gamma + \gamma'$ matrix with 2.44% dispersed M_3B_2-type boride precipitates (~ 1.4 mm). The diffusion behaviour of element B and formation mechanism of M_3B_2 boride was discussed. M_3B_2 boride particles mainly nucleated at the interface of $\gamma + \gamma'$ phases, and γ phase acted as the nucleation point of the high-energy grain boundary. Li [8] reported the microstructure evolution and mechanical properties of wide-gap brazed K417G superalloy joints with Ni-Co-Cr-Zr-B filler alloy and Ni-based additive alloy powders. The brazing experiment was conducted at 1200 °C for 30 min. B atoms uniformly diffused through the K417G alloy and additive alloy. Similarly, during brazing process segregation of element B appeared and M_3B_2 borides particles formed in the brazing seam. However, the study on the diffusion behavior of element Si in the wide-gap brazed joints is lacking.

Recommended for publication by Commission XVII - Brazing, Soldering and Diffusion Bonding.

✉ Xinyu Ren
renxy621@163.com

1   Welding and Plastic Forming Division, Beijing Institute of Aeronautical Materials, Beijing 100095, China

🌀 Springer

Fig. 1 Illustration of brazed samples, (**a**) the illustration for tensile test and (**b**) the machined samples for tensile test
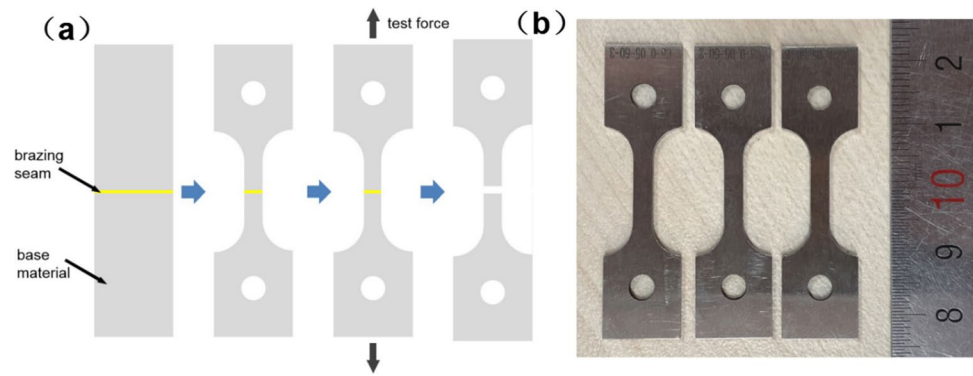
In the current study, wide-gap brazing of K417G superalloy is carried out with BNi-5 (Ni–Cr-Si) filler alloy under different holding time. The diffusion behavior of element Si into the additive alloy is characterized and the interfacial evolution mechanism is clarified.

2 Experimental procedure

In this study, the wide-gap brazing of Ni-based K417G superalloy was conducted with BNi-5 (Ni-19.0Cr-10.0Si, wt.%) filler alloy powders (~ 150 mesh).
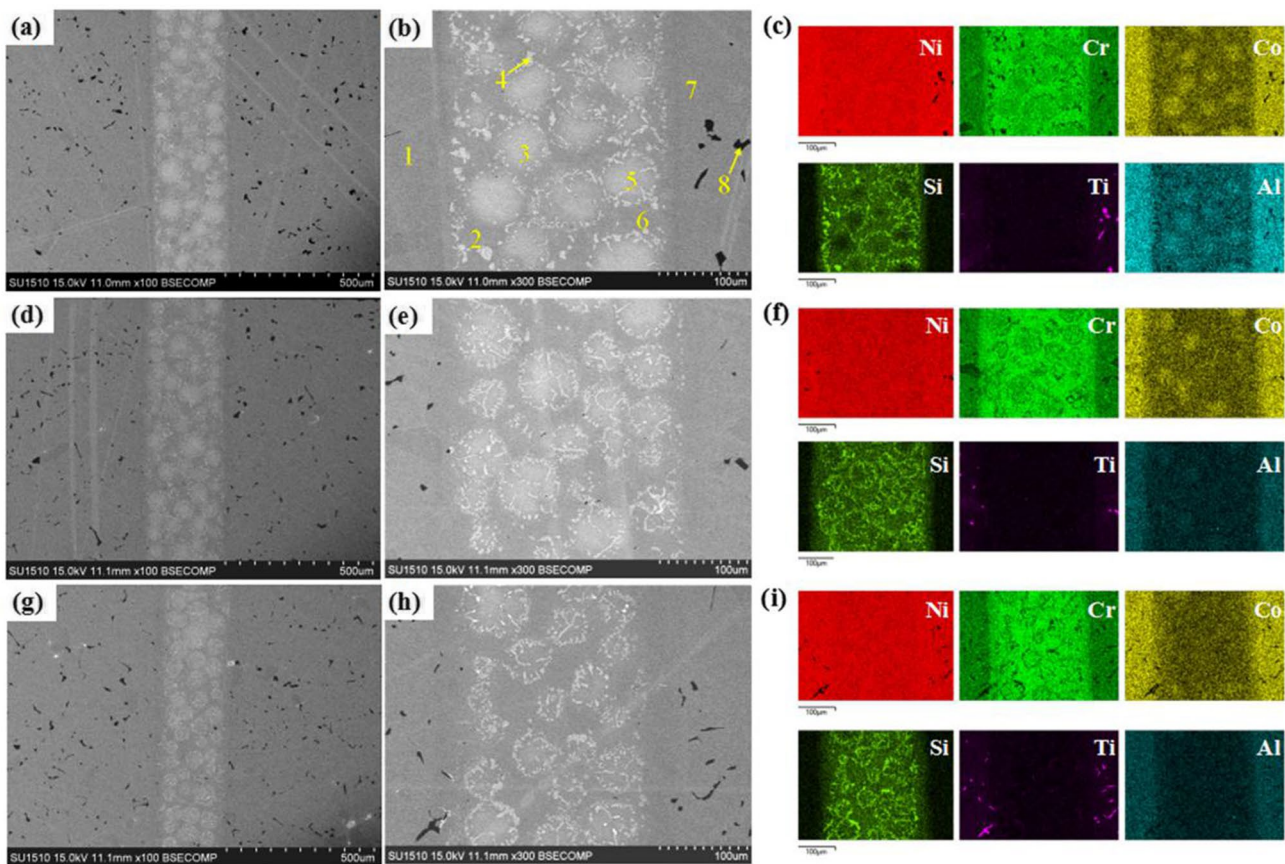

Fig. 2 Microstructure and corresponding element area distribution maps of K417G joint brazed at 1150 °C for different holding time: (**a**), (**b**) and (**c**) for 15 min; (**d**), (**e**) and (**f**) for 30 min; (**g**), (**h**) and (**i**) for 60 min

Table 1 XEDS results of the microzones denoted in Fig. 2(b)

| Micro zone	Chemical composition (at.%)								Possible phases
	Al	Si	Ti	V	Cr	Co	Ni	Mo	
1	15.38	0.14	3.86	0.98	9.36	9.32	59.06	1.9	γ/γ' phase in base material
2	7.01	11.07	1.29	0.03	16.82	4.37	58.47	0.93	γ/γ' phase in residual filler alloy
3	10.54	6.41	2.24	0.07	13.86	7.36	57.99	1.54	γ/γ' phase in superalloy particle
4	0.31	35.86	5.54	/	3.4	2.66	52.23	/	Silicides in in filler alloy
5	9.14	7.69	2.15	/	14.49	6.84	58.05	1.64	γ/γ' phase in superalloy particle
6	7.07	10.4	1.43	0	17.23	4.36	58.61	0.9	γ/γ' phase in filler alloy
7	15.46	0.11	4.6	0.8	9.53	8.96	58.7	1.84	γ/γ' phase in base material
8	0.24	0.07	70.6	4.72	1.84	0.22	1.39	20.92	Ti and Mo rich carbides
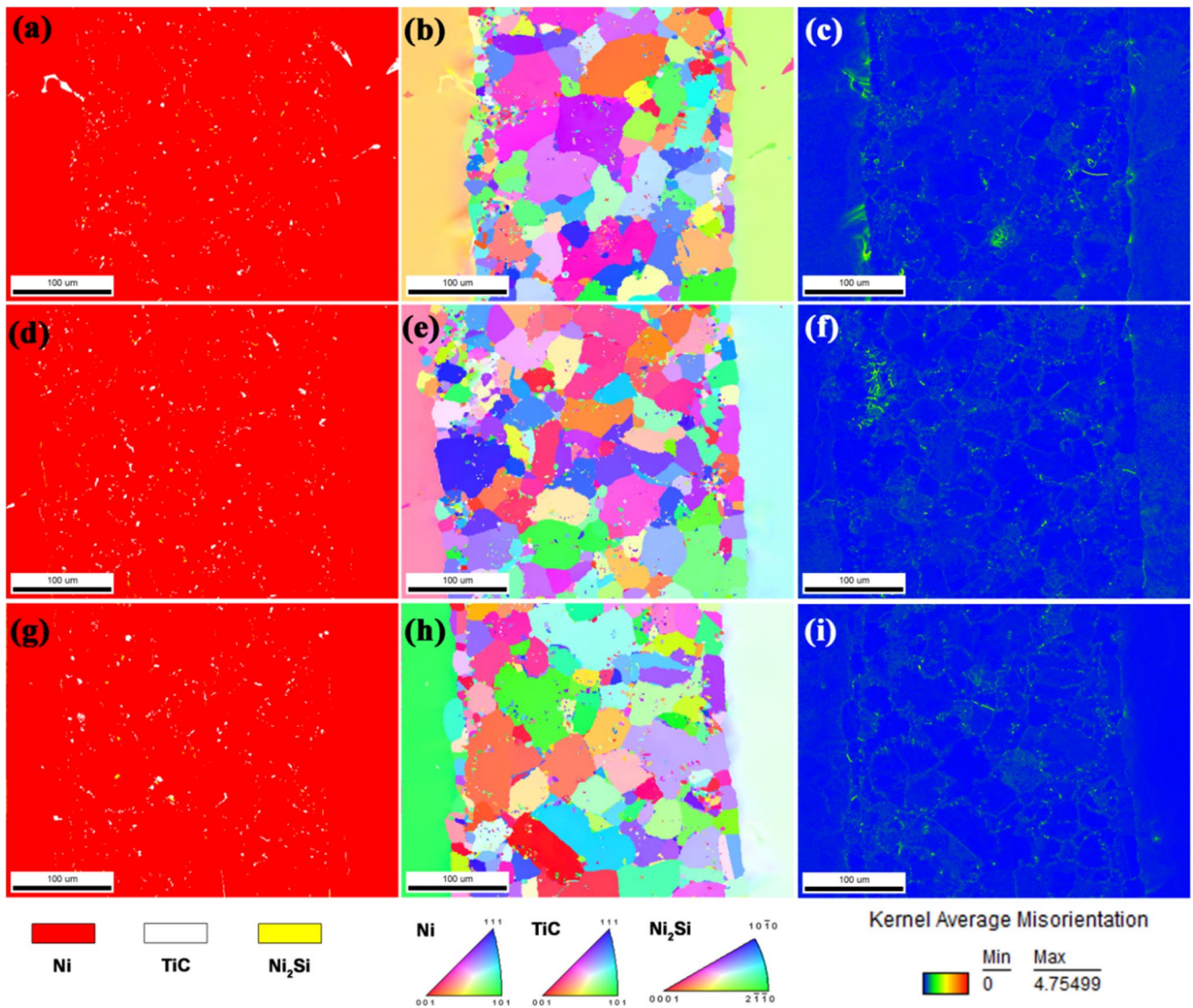
Fig. 3 EBSD phase map, inverse pole figure (IPF) and Kernel Average Misorientation (KAM) result of K417G alloy joint brazed at 1150 °C for different holding time: (a)—(c) for 15 min; (d)—(f) for 30 min; (g)—(i) for 60 min

Fig. 4 High temperature tensile strength (a) and stress–strain curves (b) of the joints brazed for different holding times
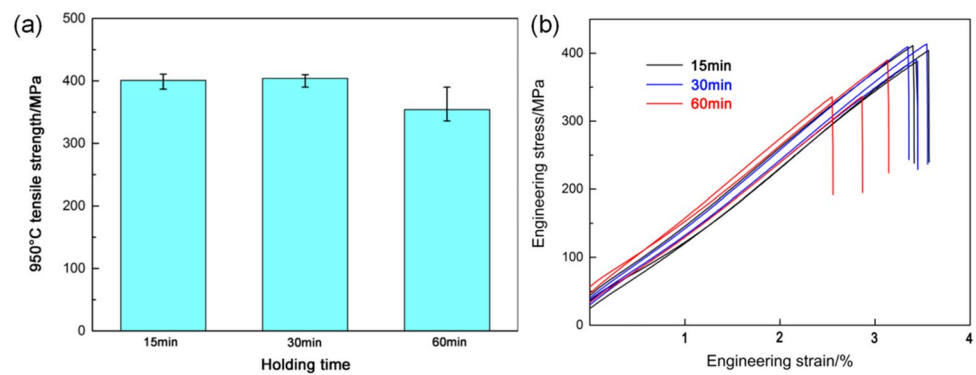
Ni-Co-Cr-Al-Ti–W-Mo-Nb superalloy powders were selected as the additive filler alloy to fill in the gap between the base alloy. The as-cast K417G base alloy was machined into the size of 24 mm×14 mm×2 mm. Prior to the brazing experiment, the surfaces to be joined were polished using SiC grit papers and then ultrasonically cleaned in acetone and ethanol solutions. The joint clearance with 0.2 mm was prepared with a fixture. The mixture paste of filler alloy and additive alloy powders was placed into the joint area. Brazing experiments were conducted at 1150 °C for three different holding time (namely 15, 30 and 60 min), followed by cooling in the vacuum furnace. The heated rate was fixed as 10 °C/min and the vacuum level was kept between 1.5×10^{-3} Pa and 6.5×10^{-3} Pa. The cross-section surface of as-brazed joints were ground and polished using the colloidal silica suspension. Polished samples were examined using scanning electron microscope (SEM) equipped with an X-ray energy dispersive spectrometer (XEDS). The brazing seam was also characterized by electron backscatter diffraction (EBSD) under 500×magnification with a consistent step size of 0.35 μm. The illustration for tensile test and machined samples for tensile test are presented in Fig. 1. Tensile strength was measured for the brazed joints at 950 °C, with a loading speed of 1 mm/min by a universal testing machine (Instron 5982). The tensile strength is the average value of three samples, similar to the methodology reported previously for the brazing of Nb_{SS}/Nb_5Si_3 composite by using Ti-Ni-Nb filler alloy [9].

3 Results and discussion

The interfacial microstructure and corresponding element area distribution maps of the K417G alloy joint brazed at 1150 °C for 15 min are presented in Fig. 2(a), Fig. 2(b) and Fig. 2(c), respectively. From the low magnification image of the brazing seam in Fig. 2 (a), it can be observed that sound joint without any voids or cracks is obtained. Meanwhile, the bright intermetallic phases are uniformly dispersed in the space between different additive superalloy

particles. The XEDS results of the microzones denoted in Fig. 2(b) are shown in Table 1. Combined with the element area distribution maps, the joint microstructure mainly consists of γ/γ' mixture phase and intermetallic phase. Zone 1 and 7 are γ/γ' matrix phases in K417G base material area [10], while zone 3 and 5 are located in the additive superalloy particle area with higher content of elements Si and Cr. This should be attributed to the element diffusion from the BNi-5 filler alloy into additive superalloy particles during the brazing process. Similar chemical concentrations are achieved for zone 2 and 6. This area is γ/γ' matrix phase in residual BNi-5 filler alloy, signifying the element diffusion of γ' former from the additive superalloy powder into residual filler alloy. Zone 4 exhibits the Si content of 35.86 at.% and is deduced to be the Ni-Si intermetallics [11]. The dark phase in the base material (zone 8) is the Ti and Mo rich carbides of the K417G substrate area[12].

When the holding time increases to 30 min, element diffusion behavior becomes stronger. As shown in Fig. 2(d), Fig. 2(e) and Fig. 2(f), element Si gradually diffuses into the additive superalloy particles and the bright silicides are gradually embedded in the residual additive superalloy particles. Meanwhile, compared with Fig. 2(c), the distribution of element Cr, Co and Al in Fig. 2(f) become more uniform. In Fig. 2(g), Fig. 2(h) and Fig. 2(i), the brazing time is further increased to 60 min and the excessive diffusion and erosion phenomenon in additive superalloy particles occurred. By comparing the joint interface under different holding time in Fig. 2, it can be observed that the brazing condition has no effect on the morphology of the Ti and Mo rich carbides in the K417G base material.

To further investigate the phase evolution behavior, EBSD analysis is carried out and the results are shown in Fig. 3. Figure 3(a), 3(d) and 3(g) present the EBSD phase maps of the joints brazed at 15 min, 30 min and 60 min, respectively. It is confirmed that the silicides formed in brazing seam is Ni_2Si phase (denoted in yellow color) and the joint interface is characterized as Ni (γ/γ' phase), TiC and Ni_2Si phases [10]. Again, the intermetallic phase

(i.e. Ni$_2$Si) is mainly distributed in the space between different additive superalloy particles. As the brazing time increased, excessive diffusion of Si occurred, causing the intermetallic particles migrate into the additive superalloy area. This finding is consistent with the previously discussed SEM and EDS mapping results. Meanwhile, from EBSD phase map, TiC phase gradually diffuses from inside towards the interface between residual filler and additive superalloy particles.

The grain orientations of the phases in the brazing seam are shown in Fig. 3(b), 3(e) and 3(h). From the grain orientation results, no obvious texture is observed. For the grain size in the brazing seam, there is little variation as the holding time increases from 15 to 60 min.

The Kernel Average Misorientation (KAM) map [13, 14] represents the average misorientation in the same grain, and it can be used to evaluate the distribution of local plastic strain and residual stress. Guo et al. [15] investigated the

Fig. 5 Fractured section of the joints brazed at 1150 °C for different holding time after high-temperature tensile test: (a) for 15 min, (b) for 30 min and (c) for 60 min
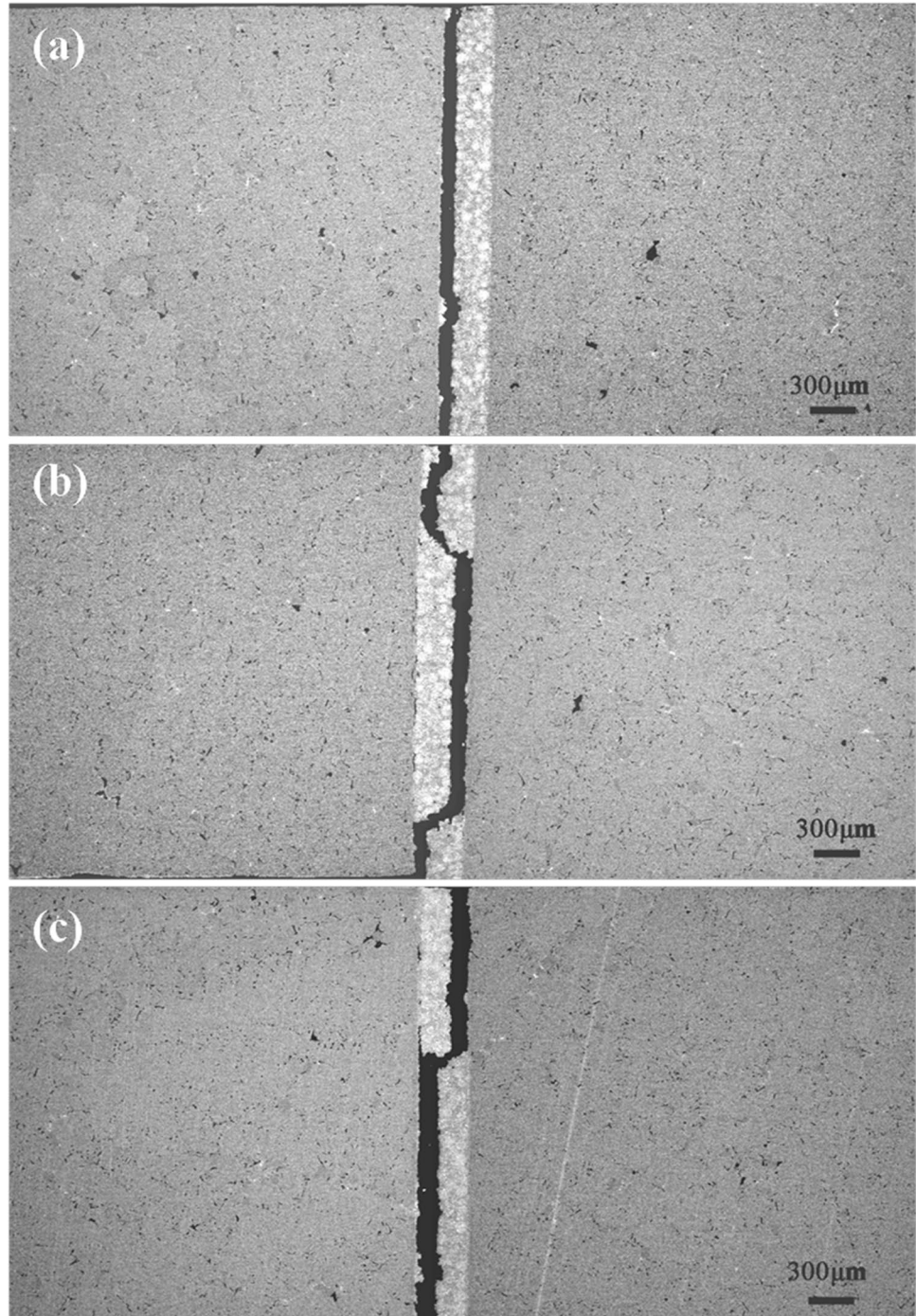
residual stress distribution of 2024-T3 and 7075-T6 aluminum dissimilar joints by neutron diffraction method and numerical simulation. The KAM results revealed the double-peak distribution of residual stress in the thermo-mechanical affected zone. According to the KAM result (Fig. 3(c), 3(f) and 3(i)), it should be noted that TiC and Ni$_2$Si intermetallic phase and the interface between the base alloy and the brazing seam area present higher residual stress.

Figure 4(a) presents the average tensile strength of the brazed joints tested at 950 °C. For the holding time of 15 min and 30 min, the average tensile strength is 401 MPa and 404 MPa, respectively. While the holding time increases to 60 min, the joint strength is decreased to 354 MPa with higher level of data dispersion. This can be attributed to the excessive diffusion and erosion of brittle intermetallic into the additive superalloy particles. The engineering stress–strain curves of the brazed joints are presented in Fig. 4(b). Considering the width of the brazing seam is only 0.2 mm, the deformation of the brazing seam is negligible. Therefore the value of engineering strain obtained by the tensile test is mainly the elastic deformation of the K417G base alloy. It should be noted that the stress–strain curves displayed in Fig. 4(b) are not corrected for machine compliance.

The fractured sections of the joints brazing at 1150 °C for different holding times after high-temperature tensile test are depicted in Fig. 5. It can be observed that during tensile test the cracks propagated along the intermetallic phases in the brazing seam and the interface between the brazing seam and the K417G base alloy area. The KAM and tensile strength results together prove that the intermetallic phase and the interface area are the weak link of the brazed joints.

4 Conclusions

In summary, the wide-gap brazing of K417G superalloy is realized by using BNi-5 filler and additive superalloy powders. The interfacial evolution and diffusion behavior are investigated. The joint interface mainly consists of γ/γ' phase, TiC and Ni$_2$Si phases. With the prolonging holding time, stronger mutual element diffusion phenomenon occurred. As a result, TiC phase diffused outwards the interface between residual filler and additive superalloy particles. Ni$_2$Si intermetallic phases gradually diffused into the additive superalloy particles, which could deteriorate the joint performance. The joints brazed at 1150 °C for 30 min exhibit highest average tensile strength of 404 MPa tested at 950 °C.

References

1. Beining Du et al (2015) Effects of grain refinement on the microstructure and tensile behavior of K417G superalloy. Mater Sci Eng, A 623:59–67
2. Li G et al (2018) Investigation of solidification and segregation characteristics of cast Ni-base superalloy K417G. J Mater Sci Technol 34:541–550
3. Henhoeffer T et al (2010) Microstructure and high temperature tensile properties of wide gap brazed cobalt based superalloy X-40. Mater Sci Technol 26:431–439
4. Xiao H et al (2008) Brazing and wide-gap Repair of X-40 Using Ni-Base Alloys. J Eng Gas Turbines Power 130:032101–032111
5. Xin J et al (2023) Ultra-high temperature brazing of C/C composite using pure Ni as filler based on eutectic reaction. Mater Lett 351:135006
6. Xiao H, Miglietti W (2012) Wide-gap braze repair of gas turbine blades and vanes-a review. J Eng Gas Turbines Power 134:010801
7. Zhun C et al (2020) M$_3$B$_2$-type borides effect on the wide-gap brazing of K417G alloy with mixed powder. J Alloy Compd 821:153431
8. Li X et al (2021) Effect of filler metal on the microstructural evolution and mechanical properties of wide gap brazed K417G superalloy joints. Vacuum 184:109967
9. Ren X et al (2020) Microstructures and joining characteristics of Nb$_{SS}$/Nb$_5$Si$_3$ composite joints by newly-developed Ti66-Ni22-Nb12 filler alloy. J Mater Sci Technol 58:95–99
10. Pouranvari M et al (2013) Phase transformations during diffusion brazing of IN718/Ni-Cr-B/IN718. Mater Sci Technol 29:980–984
11. Wenwen Li et al (2017) Joining of C$_f$/SiBCN composite with two Ni-based brazing fillers and interfacial reactions. J Mater Sci Technol 33:487–491
12. Yang YH et al (2013) Microstructure and tensile properties of nickel-based superalloy K417G bonded using transient liquid-phase infiltration. Mater Des 51:141–147
13. Allan H et al (2020) A statistical study of the relationship between plastic strain and lattice misorientation on the surface of a deformed Ni-based superalloy. Acta Mater 195:555–570
14. Shyam K et al (2021) Nucleation mechanism of hetero-epitaxial recrystallization in wrought nickel-based superalloys. Scripta Mater 191:7–11
15. Yanning G et al (2020) Study on residual stress distribution of 2024–T3 and 7075–T6 aluminum dissimilar friction stir welded joints. Eng Fail Anal 118:104911